Materials Today Bio 34 (2025) 102110

Contents lists available at ScienceDirect

Materials Today Bio

journal homepage: www.journals.elsevier.com/materials-today-bio

A bioequivalent cornea cross-linking method using photo-initiators LAP and visible light

Yi Liao [a,1], Shengmei Zhou [a,1], Andrew J. Quantock [b], Wei Li [a,g], Yuan Xu [a], Xie Fang [a,c], Robert D. Young [b], Wanling He [a], Qingjian Li [a], Houjian Zhang [a], Ruochen Wang [a], Yi Han [a], Hongwei Cheng [d,e], Wenjun Li [a], Lu Peng [a], Rongrong Zong [a], Yi Hong [f,*], Zhirong Lin [a,c,**], Zuguo Liu [a,g,h,***]

[a] Xiamen University Affiliated Xiamen Eye Center, Fujian Provincial Key Laboratory of Ophthalmology and Visual Science, Fujian Engineering and Research Center of Eye Regenerative Medicine, Eye Institute of Xiamen University, School of Medicine, Xiamen University, Xiamen, Fujian, 361005, China
[b] School of Optometry and Vision Sciences, Cardiff University, Cardiff, Wales, United Kingdom
[c] Xiamen Clinical Research Center for Eye Diseases, Xiamen Key Laboratory of Ophthalmology, Fujian Key Laboratory of Corneal & Ocular Surface Diseases, Xiamen Key Laboratory of Corneal & Ocular Surface Diseases, Translational Medicine Institute of Xiamen Eye Center of Xiamen University, Xiamen, Fujian, 361102, China
[d] Zhuhai UM Science & Technology Research Institute, University of Macau, Macau SAR, 999078, China
[e] State Key Laboratory of Vaccine for Infectious Diseases, Xiang an Biomedicine Laboratory, National Innovation Platform for Industry-Education Integration in Vaccine Research, State Key Laboratory of Molecular Vaccinology and Molecular Diagnostics, School of Public Health, Xiamen University, Xiamen, 361102, China
[f] Department of Sports Medicine of the Second Affiliated Hospital, and Liangzhu Laboratory, Zhejiang University School of Medicine, Hangzhou, Zhejiang, China
[g] Department of Ophthalmology, Xiang'an Hospital of Xiamen University, Xiamen, Fujian, 361005, China
[h] Department of Ophthalmology, The First Affiliated Hospital of University of South China, Hengyang, Hunan, 421001, China

ARTICLE INFO

Keywords:
Corneal cross-linking
Lithium phenyl-2,4,6-trimethylbenzoylphosphinate (LAP)
Visible light
Collagen
Biocompatibility

ABSTRACT

Although cell-encapsulating hydrogels are of tremendous interest in regenerative medicine, few of them have been used in clinics and rarely used natural extracellular matrices as polymer precursors. One successful example is to use riboflavin (RF)/ultraviolet A (UVA) to cross-link corneal collagen, which has been used in clinics to halt disease progression in patients with corneal ectatic diseases. However, high-energy UVA and its action on RF cause tissue damage, particularly irreversible endothelium loss, and thus standard RF/UVA protocol may have limitations in treating patients at the advanced stage with thin cornea. Photo-initiators lithium phenyl-2,4,6-trimethylbenzoylphosphinate (LAP) has high efficiency under visible 405 nm light, and is widely applied in 3D bioprinting to cross-link synthesized monomers. Here, we introduced a new strategy to cross-link cornea using LAP and visible light (VL). The LAP/VL protocol could effectively increase corneal stiffness with equivalent efficiency to the RF/UVA protocol in both porcine and rabbit cornea. As LAP and VL were used, the loss of corneal endothelial and stromal cells was minimized, and epithelial wound healing and stromal cell repopulation were accelerated. In summary, we propose that the LAP/VL protocol is an effective and safe alternate for cornea CXL with advantages for relatively thin cornea. Our study also expands the application scope of LAP, indicating it is a suitable photocatalyst for *in situ* natural extracellular matrices CXL.

* Corresponding author.
** Corresponding author. Xiamen University Affiliated Xiamen Eye Center, Fujian Provincial Key Laboratory of Ophthalmology and Visual Science, Fujian Engineering and Research Center of Eye Regenerative Medicine, Eye Institute of Xiamen University, School of Medicine, Xiamen University, Xiamen, Fujian, 361005, China.
*** Corresponding author. Xiamen University Affiliated Xiamen Eye Center, Fujian Provincial Key Laboratory of Ophthalmology and Visual Science, Fujian Engineering and Research Center of Eye Regenerative Medicine, Eye Institute of Xiamen University, School of Medicine, Xiamen University, Xiamen, Fujian, 361005, China.
E-mail addresses: liaoyilori@xmu.edu.cn (Y. Liao), 1812661977@qq.com (S. Zhou), QuantockAJ@cardiff.ac.uk (A.J. Quantock), weili@xmu.edu.cn (W. Li), xuyuan_0210@163.com (Y. Xu), 307082411@qq.com (X. Fang), Youngrd@cardiff.ac.uk (R.D. Young), hewan0000@163.com (W. He), liqingjianvip@163.com (Q. Li), 1053545691@qq.com (H. Zhang), ruochen_wang@yeah.net (R. Wang), hanyixmu@foxmail.com (Y. Han), zumri.hwcheng@um.edu.mo (H. Cheng), liwenjun@xmu.edu.cn (W. Li), penglu@xmu.edu.cn (L. Peng), zrr617@163.com (R. Zong), yihong@zju.edu.cn (Y. Hong), zlin15@xmu.edu.cn (Z. Lin), zuguoliu@xmu.edu.cn (Z. Liu).
[1] These two authors contributed equally to this work.

https://doi.org/10.1016/j.mtbio.2025.102110
Received 19 March 2025; Received in revised form 26 June 2025; Accepted 16 July 2025
Available online 17 July 2025

1. Introduction

The cornea is the primary refractive medium of the eye, which works with the overlying tear film to control about 2/3 of optical power [1]. The transparency, regularity, and shape of the cornea affect its function. One of the determinants of the cornea's shape is the collagen matrix's mechanical properties in the stroma. Corneal ectasia diseases, including keratoconus, post-LASIK (Laser-assisted In Situ Keratomileusis) ectasia, and pellucid marginal degeneration (PMD), usually lead to astigmatism and progressive loss of vision due to the thinning of cornea stroma and resultant reduction in corneal mechanical strength [2]. Thus, strategies to maintain and, even better, increase corneal stroma strength are beneficial for these patients.

The stroma is the thickest layer of cornea, mainly composed of collagen fibrils. Previously, 3-dimensional mapping demonstrated that the alignment and macrostructural organization of collagen fibrils control the mechanical stiffness and shape of the cornea [3]. A reduction in interconnections between the collagen fibrils and/or the neighboring proteoglycans is considered to contribute to the pathogenesis of keratectasia [4]. Traditionally, induction of cross-links in corneal tissue by riboflavin (RF, here stands for riboflavin-5′-phosphate)/ultraviolet A (UVA) is used as a conservative treatment to increase the stiffness of the cornea with ectasia diseases [4b,5]. Although the introduction of corneal cross-linking (CXL) significantly decreases the incidence of corneal transplantation [6], multiple complications limit its application in patients. One primary concern is the use of high-energy UVA for CXL, which may induce reactive oxygen species (ROS) and potentially damage corneal cells [5b,7]. Furthermore, when UVA irradiates RF, it also generates ROS, which exert lethal effects in corneal cells (particularly endothelial cells), including DNA damage and membrane peroxidation, ultimately leading to apoptosis and necrosis [8]. Thus, postoperative complications after CXL, such as corneal edema, haze, and scarring, may arise.

Recently, multiple photocatalysts have been discovered, purified, and/or synthesized to cross-link collagens for biochemical purposes [9]. Additionally, the development of green chemistry, which fosters sustainable chemical synthesis using non-hazardous and environmentally friendly reagents, leads to the creation of several water-soluble photo--initiators with photopolymerization capabilities under visible light [10]. Specifically, a synthesized photo-initiator lithium phenyl-2,4,6-trimethylbenzoylphosphinate (LAP) shows good stability in the water and improved spectroscopic properties with absorption characteristics in the visible light (VL) range [11], and thus may reduce the chance of tissue damage. In addition, several studies have demonstrated that LAP can mediate efficient radical photopolymerization in tissue engineering using synthesized monomers with relatively low cytotoxicity [10,12]. Accordingly, in this study, we investigated a LAP/VL protocol as an alternative to the RF/UVA protocol to cross-link native corneal collagen *in vivo*. Our results showed that LAP/VL could effectively cross-link collagen fibrils/possibly proteoglycans, increase corneal stiffness in enucleated porcine eyes and adult rabbits under the same light intensities used in the RF/UVA protocol. As expected, the LAP/VL protocol significantly reduced corneal tissue damage in rabbits. Our results strongly indicated that a LAP/VL protocol could be a promising and safe alternate for patients with corneal ectasia diseases.

2. Materials and methods

2.1. Materials

Synthesis of the photo-initiator: Dimethyl phenylphosphonite (Ourchem) was reacted with 2,4,6-trimethylbenzoyl chloride (Sigma-Aldrich) via a Michaelis–Arbuzov reaction. At room temperature and under argon gas, 3.2 g (0.018 mol) of 2,4,6-trimethylbenzoyl chloride was added dropwise to an equimolar amount of continuously stirred dimethyl phenylphosphonite (3.0 g). The reaction mixture was stirred for 18 h whereupon a fourfold excess of lithium bromide (Aladdin, 6.1 g) in 100 mL of 2-butanone (Sinopharm Chemical Reagent) was added to the reaction mixture from the previous step, which was then heated to 50 °C. Ten minutes later, a solid precipitate had formed. The mixture was cooled to ambient temperature, allowed to rest for 4 h, and then filtrate. The filtrate was washed and filtrate three times with 2-butanone to remove unreacted lithium bromide and excess solvent was removed by vacuum.

Lithium phenyl-2,4,6-trimethylbenzoylphosphinate (LAP) powder was prepared in a normal saline solution to reach a final concentration (w/v). The riboflavin (RF) solution was purchased from ParaCel (Avedro, United States). It was composed of 0.25 % (w/v) riboflavin with hydroxypropyl methylcellulose, ethylenediaminetetraacetic acid (EDTA), and benzalkonium chloride (BAC).

2.2. Corneal cross-linking procedure

Porcine or rabbit corneal epithelium was removed with an epithelial scraper, and 2–3 drops of the cross-linking solutions were applied to the cornea every 3 min for 15 min. Afterward, the cornea was irradiated with ultraviolet (UVA, 365 nm) or visible light (VL, 405 nm) at 4.5 mW/cm^2 for 20 min, and the cross-linking reagents were added at the same frequency until the irradiation was completed. After cross-linking, the ocular surface and surrounding area were rinsed with normal saline solution.

2.3. Animal experiments

Male New Zealand white rabbits without clinically observable ocular surface abnormalities (weight 2.3–2.6 kg) were purchased from Chedundongwu (Shanghai, China) and housed in Xiamen University Laboratory Animal Center (Xiamen, Fujian, China) for 2 weeks before the experiments. C57BL/6 mice (~8 weeks) were purchased from Xiamen University Laboratory Animal Center. This study was approved by the Experimental Animal Ethics Committee of Xiamen University (No. XMULAC20230110) and was performed according to the standards of the Association for Research in Vision and Ophthalmology Statement for the use of Animals in Ophthalmic and Vision Research. Rabbits were randomly assigned into RF/UVA and LAP/VL groups. They were anesthetized with an intra-muscular injection of xylazine hydrochloride injection (10 mg/kg, Shengda, Jilin, China) and 10 % chloral hydrate (1.5 mL/kg, Zancheng, Tianjin, China) and cross-linking procedures were performed. The left eye was used for cross-linking for each rabbit, while the right eye was used as control.

2.4. Draize's eye test

Four Male New Zealand white rabbits were used to test *in vivo* ocular irritation of LAP solution. According to ARVO guidelines, only one eye (left eye) was chosen for testing LAP solution (0.25 % w/v), and the other eye instilled with solvent (normal saline) was used as a negative control. 2–3 drops of LAP solution were applied to the ocular surface (including cornea and conjunctiva) every 3 min for a continuous 35 min. After 1 h of the last dosing, eyes were periodically (1 h, 1 d, 2 d, 3 d, 4 d, and 5 d) observed for any injuries or signs and symptoms in the cornea, iris, conjunctiva by slit lamp or *in vivo* confocal microscope.

2.5. Cell cultures

Primary human corneal stromal cells (HCSC) were isolated from the central cornea of keratoconus patients after keratoplasty. The entire research procedure adhered to the principles in the Declaration of Helsinki and was approved by the Medical Ethics Committee of Xiamen University (XDYX202311K73). After removing the endothelium, the cornea was digested with DispaseII(Cat.No.: D4693-1G, Lot No.: BCCB3250, Sigma, Shanghai, China) at 4 °*C* for 12 h, and the epithelium

was peeled off. Afterward, the corneal stroma was digested with collagenaseIat 37 °*C* for 6 h, and the digested tissue was cultured in DMEM with 10 % FBS and 1 % P/S for 3–4 days. Later, adherent cells were passaged and used for *in vitro* cell experiments.

2.6. Cell counting kit-8 (CCK-8) analysis

HCSC were seeded in 96-well plates with ~70 % confluency. LAP or RF with indicated concentrations were added into a culture medium and incubated with cells for 24, 48, and 72 h. Then, 10 μL CCK-8 solution (Cat No.: RM02823, Lot No.: 9900000006, Abclonal, Wuhan, Hubei, China) was added into each well and incubated cells for 4 h. Absorbance at 450 nm was measured with a Bio Tek ELX800 Microplate Reader (Bio-Tek Instruments, Winooski, VT, USA).

2.7. Live/dead cell staining

To evaluate cytotoxicity, HCSC were seeded in 96-well plates at a density of 1.5×10^4 cells per well. After 24 h treatment with 0.25% (w/v) LAP or 0.25% (w/v) RF, cells were washed twice with DMEM medium. Then Calcein-AM and propidiuim iodide were added and incubated in the dark for 30 min according to the manufacturer's instruction (Live and Dead Cell Double Staining Kit, Cat No.:KTA1001, Lot No.: ATYD21161, Abbkine Inc, USA). Cell viability was observed under a fluorescence microscope (Ts2, Nikon, Japan).

2.8. Histological analysis, Masson staining, and immunofluorescence staining

The corneal samples were dissected around the limbus and fixed in 4 % paraformaldehyde solution for at least 24 h. Then, the tissue was embedded in paraffin, cut into 5 μm slices, and stained with Hematoxylin and eosin (H&E; Cat. No.:DH0006, Lot No.: 0315A22, Leagene, Beijing, China) or Masson's trichrome (Cat. No.: D026-1-1, Lot No.:20230104, Nanjing Jiancheng Bioengineering Institute, Nanjing, Jiangsu, China). Staining procedures were performed according to the supplier's instructions.

For immunofluorescence staining, the tissue sections on slides were boiled in antigen retrieval solution (Cat. No.: MVS-0101, Lot No.: 2401160432a, MXB Biotechnologies, Fuzhou, Fujian, China) in a microwave oven for 30 min. 0.2 % (v/v) Triton X-100 solution was used to permeate the membrane for 20 min, and then the tissues were blocked with 2 % BSA for 1 h. The sections were incubated with anti-8-OHdG antibody (1:50, Cat. No.: sc-39387, Lot No.: J0623, Santa Cruz Biotechnology, Santa Cruz, USA, RRID: AB_2892631) and anti-γH2AX (1:200, Cat. No.:05-636-I, Lot No.:3429624, Millipore, Beijing, China, RRID: AB_2755003) at 4 ° C overnight. Next, sections were incubated with anti-mouse secondary antibodies (488, 1:200, Cat. No. A21022, Lot No.: 2659299, ThermoFisher, USA, RRID: AB_141607) and Hoechst for 1 h. The images were obtained using a Zeiss LSM 880 confocal microscope.

2.9. Wholemount staining

After the CXL procedures, rabbits were sacrificed, and the central cornea was harvested and fixed in 4 % paraformaldehyde for 15 min. The central cornea was washed three times each for 5 min with 1xPBS, and then stained with primary antibodies: ZO-1 (1:100, Cat. No.: 33–9100, Lot No.: YC368286, Invitrogen, RRID: AB_87181), Na^+-K^+ ATPase (1:100, Cat. No.: ab76020, Lot No.: 1007907-32, Abcam, RRID: AB_1310695) at 4 ° C overnight. The next day, the cornea was washed with 1xPBS and then incubated with anti-rabbit (594, 1:200, Cat. No.: A11012, Lot No.: 2616076, Invitrogen, RRID: AB_141359) or anti-mouse (488, 1:200, Cat. No. A21022, Lot No.: 2659299, ThermoFisher, USA, RRID: AB_141607) secondary antibodies for 1 h. The images were obtained using a confocal scanning microscope (Fluoview 1000; Olympus, Tokyo, Japan).

2.10. Light transmission examination

Corneal transparency was examined by measuring the light transmittance using a microplate reader. Fresh corneal samples were harvested following cross-linking surgery. The rabbit central cornea was excised and trimmed into circular buttons that matched the dimensions of the wells in a 96-well plate, with the endothelial side facing upward and the cornea entirely flattened, adhering to the base of the wall. The microplate reader was calibrated to measure absorbance (A) across a wavelength range of 200–1000 nm. Transmittance (T) value was calculated using the following formula:

$$T(\%) = \frac{1}{10^A} \times 100$$

2.11. AFM analysis

After application of the CXL procedure, the cornea was carefully washed with normal saline to remove impurities attached to the surface, but with care not to stretch or compress the tissue. The central 7 mm disc was removed and fixed it in a 6 cm dish with cyanoacrylate glue with the corneal epithelium side facing up. PBS was added to the dish to simulate the *in vivo* environment.

The mechanical strength of the corneal surface was measured by AFM (Bruker Nanowizard4, American). A Bruker NP-010-D-22 μm SiN tipless cantilever (Tip radius = 11 μm; spring constant = 0.038 N/m) was chosen. AFM would draw the force curve at a certain point, and the Young's Modulus was calculated using AFM analysis software according to Hertz model:

$$F = \frac{4E\sqrt{R}}{3(1-\nu^2)}\delta^{\frac{3}{2}}$$

F stands for loading force, R for the probe tip radius, ν for the Poisson ratio, and δ for the indentation depth.

The test was conducted in 5 areas designated as above, below, left, right, and center of each corneal button. Three points were randomly selected in each region to obtain the force curve, and at least six curves were collected at each point. The Young's modulus of each point is the average Young's modulus of the collected force curves, and the hardness of each region is represented by the average Young's modulus of three points.

To measure the Young's modulus after CXL, 7 cornea samples were used for the CTRL group, 6 for the RF/UVA group, and 6 for the LAP/VL group. To quantify the long-term maintenance of corneal stiffness after CXL, 4 cornea samples were used for the CTRL group, and 5 were used for the LAP/VL group.

2.12. Stress-strain analysis

After the cross-linking procedure, rabbits were sacrificed, and a special double-edged knife was used to excise a 4 mm × 10 mm corneal strip from the center of the cornea. Corneal strips were immediately preserved at 4 °C in sealed containers after harvesting and used within 6 h. The corneal strip was fixed vertically in the jaws of the equipment (microtester 5948, Instron ITW, USA). The tensile speed was 2 mm min-1, and the pre-cycling tensile load was 0.5 N. The displacement and load were adjusted to zero after pre-load to 0.5 N. The tensile displacement was 1 mm at a speed of 2 mm min^{-1} and then was returned to zero at the same speed. Three cycles were performed for each corneal strip with an interval of 30 s. Finally, the strip was stretched to 120 % at a loading speed of 2 mm min^{-1}, and a stress-strain curve was generated to calculate the slope of the curve as Young's modulus. Uniaxial tensile testing was performed in an ambient atmosphere at 20 °C and a relative humidity of 50–60 % in air, and each test was completed within 5 min to

minimize tissue dehydration.

2.13. Enzymatic resistance analysis

After the cross-linking procedure, rabbits were sacrificed, and the central 8 mm diameter corneal button was harvested. The corneal button was placed in collagenase I solution (650 U/mL, Cat. No.: 40507ES60, Lot No.:C6316220, YEASEN, Shanghai, China) with constant shaking (110 rpm, 37 ° C), and the weight of the remaining corneal tissue was measured after 6 h of enzyme digestion.

2.14. Transmission electron microscopy (TEM) and quantification

Cornea tissue was quickly immersed in 2.5 % (v/v) glutaraldehyde fixative solution for 2–4 h at 4 ° C, then washed in 1xPBS thrice for 15 min each time and post-fixed in 1 %(v/v) osmium tetroxide. Subsequently, the cornea was dehydrated with 30 % and 50 % ethanol, and stained with uranyl acetate in 70 % ethanol, followed by dehydration in a graded ethanol series. The cornea was embedded in resin, and sections were cut on an ultramicrotome, mounted on nickel grids, and stained with Renold lead citrate. The images were acquired using transmission electron microscopy (HT-7800, HITACHI, Japan) at 80 kV. Fibril diameter was measured with Image J (RRID: SCR_003070), and fibril diameter distribution was mapped with Origin 2022 (https://www.originlab.com/2022)(RRID: SCR_002640)

2.15. Scanning electron microscopy (SEM)

Cornea tissue was quickly fixed in cold 2.5 %(v/v) glutaraldehyde fixative solution, and rinsed with phosphate buffer three times. Next, samples were sequentially dehydrated in 30 %, 50 %, 70 %, 90 % and 100 % ethanol. Specimens were transferred into Critical Point Dryer (CPD, Leica CPD300) holding devices containing 100 % ethanol, and quickly transferred into the CPD chamber. The chamber was sealed to start running the CPD. When CPD was finished, specimens were removed from the CPD device and mounted using double-sided sticky carbon tape on aluminum SEM mounting stubs. The samples were sputter-coated (Jeol, JFC-1600, Japan) with a thin layer of platinum at approximately 6 nm for 60 s with a sputter current of 30 mA. The accelerating voltage is 5 kV for SEM imaging using ThermoFisher Helios 5 UC scanning electron microscope.

2.16. Wound healing assay

The corneal epithelium of rabbits was removed within a diameter of 8 mm in the center, and the above-mentioned cross-linking procedure was applied to the corneal surface. Afterward, ofloxacin eye ointment (CISEN, China) and tobramycin dexamethasone eye ointment (NOVARTIS, USA) were applied twice daily. Starting from 24 h after cross-linking, corneal epithelial integrity indicated by fluorescein staining and stroma thickness were evaluated with a slit lamp (BQ900; Haag-Streit AG, Koeniz, Switzerland) every day.

2.17. In vivo corneal confocal microscopy

Rabbits were anesthetized, carbomer gel was added to the lens cap, and the rabbit's central cornea was positioned in close contact with the cap. The images of corneal epithelium, endothelium, and stroma at different depths were recorded by *in vivo* corneal confocal microscopy (IVCM, HRT3/Rostock Cornea Module, Heidelberg Engineering Inc, Germany).

2.18. Anterior segment optical coherence tomography (AS-OCT)

Rabbits were anesthetized, and corneal stroma pictures were obtained using AS-OCT (Visante OCT, Carl Zeiss Meditec, Germany) according to previously published methods [13].

2.19. Statistical analysis

The collagen fibril diameter data were presented as median ± standard deviation (S.D.) values, and other data were presented as mean ± S.D. values. Statistical analysis was performed with GraphPad Prism software 9.0 (http://www.graphpad.com/, RRID: SCR_002798) by one-way/two-way ANOVA with post-hoc Bonferroni analysis. The particle size distribution plots and stress-strain curves were generated with Origin 2022 (RRID: SCR_002640).

3. Results

3.1. Preparation and characterization of LAP

LAP powders were synthesized in-house, and its structure (Fig. 1a) and purity were verified by ^{1}H nuclear magnetic resonance (NMR) (Fig. S1). To prepare a solution suitable for cornea CXL, LAP was dissolved in normal saline at a final concentration of 0.25 % (w/v). As shown in Fig. 1b, LAP was completely dissolved in normal saline without precipitation.

3.2. Ex vivo cross-linking capabilities of LAP in porcine cornea under visible light

It was shown previously that sunlight, ultraviolet A (UVA), and visible light (VL) all could cross-link porcine cornea *in vitro* in combination with RF infiltration [4]; however, VL fails to achieve the same corneal CXL strength as UVA [4]. Considering the fact that LAP has good absorbance under VL wavelength 405 nm, we directly used fresh cadaver porcine eyeballs to study whether LAP could cross-link corneal stroma under VL with the equivalent effectiveness as RF/UVA treatment. To compare the CXL outcomes with RF/UVA protocol used in clinics, about 8 mm diameter of epithelium in the central cornea was removed, and solutions (Group 1: CTRL, normal saline; Group 2: 0.1 % (w/v) LAP in saline; Group 3: 0.25 % (w/v) LAP in saline; Group 4: 0.25 % (w/v) commercial RF) were instilled to soak the corneal stroma for 15 min. Afterward, CXL was performed using 4.5 mW/cm^2 light to irradiate the eyeballs for 20 min, and thus achieved a total dose of 5.4 J/cm^2. While UVA was used for RF group, VL was used for LAP groups. Immediately after CXL, central corneal buttons were collected for further analysis.

Firstly, the optical properties of the cornea after CXL were examined. Besides the RF-soaked cornea turning yellow after treatment, corneal transparency among the 4 groups had no observable differences (Fig. S2a), indicating LAP/VL CXL could preserve corneal transparency. In the untreated control (CTRL) group, corneal stroma was uniformly stained blue after Masson's trichrome staining (Fig. S2a). Regular alignment of collagen lamellae was shown by both Masson's and H&E staining (Fig. S2a). After CXL, the gaps between collagen layers were shrunken in the 0.1 %(w/v) LAP/VL treated group, and were further reduced when 0.25 %(w/v) LAP/VL or RF/UVA was used (Fig. S2a). Moreover, the staining color in the anterior 1/4 part of corneal stroma became lighter after CXL (Fig. S2a), either due to the shrinkage of interfibrillar space or the formation of new links between lysine residues of collagen fibrils. These results indicated that the LAP/VL protocol could cross-link corneal stroma *in vitro*.

The purpose of corneal CXL is to increase corneal stiffness, which is accomplished by forming chemical covalent bonds at the surface of collagen fibrils and the surrounding proteoglycans [14]. Accordingly, the CXL effect at the corneal stromal surface was evaluated by atomic force microscopy (AFM) through indentation (Fig. S2b). For the CTRL group, the Young's modulus was 3 ± 1 kPa (Fig. S2c, Table S1). When the cornea was cross-linked with 0.1 % LAP under VL, the corneal surface stiffness was increased by 2 folds to 6 ± 4 Kpa after CXL, and the

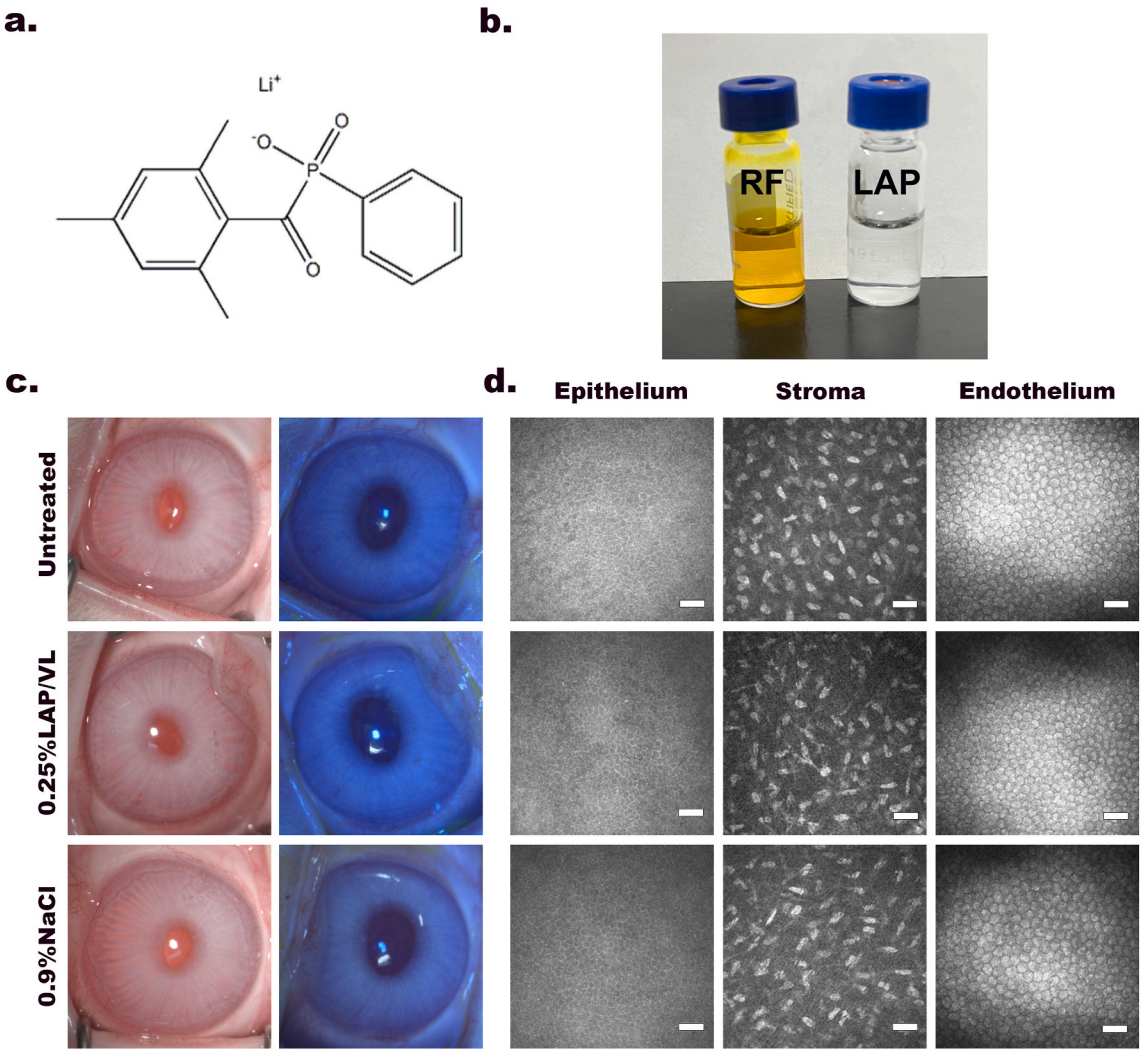

Fig. 1. (a) Chemical structure of LAP. (b) Photo pictures of riboflavin solution and LAP solution. (c) Slit-lamp images of rabbit cornea after different treatments. (d) *In vivo* confocal imagining of cornea epithelium, stroma (at ~150 μm) and endothelium after different treatments (scale bar = 50 μm).

stiffness was increased by 3 folds to 9 ± 5 Kpa when 0.25 % LAP was used (Fig. S2c, Table S1). The CXL results of the 0.25 % LAP/VL protocol tied well with the RF/UVA protocol, and the corneal surface stiffness in RF/UVA groups was slightly but not significantly higher than 0.25 % LAP/VL group (RF/UVA group: 10 ± 4 KPa) (Fig. S2c, Table S1). These mechanical force measurement results further proved that LAP/VL could cross-link cornea stroma.

3.3. *In vivo ocular irritation test of LAP*

Before testing the CXL effectiveness of the LAP/VL protocol *in vivo*, Draize's test was used to test if LAP solution could cause anterior ocular segment irritation in New Zealand white rabbits. 0.25 %(w/v) LAP solution (selected based on *in vitro* porcine experiments) was instilled to the rabbit ocular surface for 35 min with 2–3 drops every 3 min. Slit-lamp examination suggested that the cornea and conjunctiva were almost normal after treatment, and the fluorescein staining showed that the corneal epithelium integrity was not affected (Fig. 1c). A slight irritation with mild circumcorneal hyperemia involving the iris was observed in one LAP-treated eye, which was given a score of 1 in iris section (Table 1). Additionally, signs or symptoms of ocular irritation (including mild redness and chemosis) were observed at 24 h after treatment (Table 1), which were recovered at 2 d (data not shown). Subsequently, in order to quantify the ocular irritation potential of LAP, the maximum mean total scores (MMTS) were calculated by summarizing the scores in Table 1. For the 0.25 % LAP solution, the MMTS at 24 h was 2.75 (<5), whereas the 0.9 % NaCl solution (normal saline) showed an MMTS of 2 (<5) (Table 2). The MMTS values indicated both solutions were classified as non-irritant [15]. *In vivo* corneal confocal microscope (IVCM) revealed no obvious changes in corneal epithelium, stroma, and endothelium at 24 h after treatment (Fig. 1d). These results suggested the safety of LAP for ocular surface application.

3.4. *In vivo cross-linking effects of LAP in rabbits under visible light*

Next, New Zealand white rabbits were used as animal models to test the CXL effectiveness of the LAP/VL protocol *in vivo*. Based on the results obtained from porcine eyes, 0.25 % LAP was selected for *in vivo* experiments. Immediately after CXL procedures, rabbits were sacrificed, and cornea buttons were collected. Similar to the results in porcine corneas, the corneal transparency was not altered after LAP/VL CXL, yet cornea buttons turned yellow after soaking with RF with a reduced light transmittance at wavelengths below 600 nm (Fig. 2a and b). When cornea buttons from CTRL, 0.25 % LAP/VL and RF/UVA groups were placed on the same platform with the epithelium side facing down, LAP and RF groups had smaller contact areas and fewer wrinkles (Fig. 2a), suggesting that CXL is effective in increasing corneal stiffness. H&E staining of cornea stroma showed a more compact and neat alignment of

Table 1
Weighted scores for eye irritation test by 0.25 %LAP/VL and 0.9 % NaCl.

Lesion in the Treated Eyes	Individual Score for Eye Irritation							
	0.25 %LAP/VL				0.9 % NaCl			
	Rabbits#				Rabbits#			
	1st	2nd	3rd	4th	1st	2nd	3rd	4th
Cornea								
I. Opacity (Degree of density)	0	0	0	0	0	0	0	0
II. Area of cornea	4	4	4	4	4	4	4	4
Total scores = (I × II × 5) =	0	0	0	0	0	0	0	0
Iris								
I. Lesion values	0	0	0	1	0	0	0	0
Total scores = (I × 5) =	0	0	0	5	0	0	0	0
Conjunctiva								
I. Redness	0	0	1	1	0	1	0	1
II. Chemosis	0	0	0	1	0	0	0	1
III. Mucoidal discharge	0	0	0	0	1	0	0	0
Total scores = (I + II + III) × 2 =	0	0	2	4	2	2	0	4

Table 2
Maximum Mean Total Score (MMTS) calculations for the tested formulations as per the obtained scores.

0.25 %LAP/VL						
Animal #	1st	2nd	3rd	4th	SUM	Average (SUM/4)
Cornea	0	0	0	0	0	0
Iris	0	0	0	5	5	1.25
Conjunctiva	0	0	2	4	6	1.5
SUM total =	0	0	2	9	11	2.75
0.9 %NaCl						
Animal #	1st	2nd	3rd	4th	SUM	Average (SUM/4)
Cornea	0	0	0	0	0	0
Iris	0	0	0	0	0	0
Conjunctiva	2	2	0	4	8	2
SUM total =	2	2	0	4	8	2

collagen lamellae after CXL (Fig. 2c). Changes in the tertiary structure of collagen fibrils induced by CXL create steric hindrance, which prevent the access of collagenases to their specific digestion sites, and thus increase the resistance of cornea to enzymatic digestion [16]. Therefore, cornea buttons of the same size from the three groups were digested with Collagenase I to further evaluate CXL effects and cornea rigidity. After 6 h of incubation, residual cornea tissues from the LAP/VL and RF/UVA groups were about 5-fold heavier than those from the CTRL group, suggesting a significantly slower rate of cornea dissolution after CXL ($p < 0.001$ for both LAP/VL vs. CTRL and RF/UVA vs. CTRL, Fig. 2d).

When the corneal stroma surface stiffness was measured by AFM, Young's modulus for CTRL cornea was 2 ± 1 kPa. This value was increased to 8 ± 8 kPa in the LAP/VL group and 7 ± 7 kPa in the RF/UVA group ($p = 0.0005$ for LAP/VL vs. CTRL; $p = 0.0084$ for RF/UVA vs. CTRL; $p = 0.6693$ for LAP/VL vs. RF/UVA; Fig. 2e–Table 3). To quantify the overall changes of corneal elasticity after CXL, standard stress-strain tests were used (Fig. 2f). When central cornea strips were subjected to force and displacement measurements, the stress-strain curves showed that the stress applied to generate similar corneal deformation was about 2-fold higher in CXL groups than the CTRL group (Fig. 2g). Consistent with the results obtained by AFM indentation, LAP/VL treated corneas had slightly higher Young's modulus than RF/UVA treated corneas, yet the differences were not statistically different (Fig. 2h–Table 4).

Additionally, CXL could modify the ultrastructure of collagen fibrils, including size, spacing, and spatial arrangement [17]. Accordingly, the corneal stroma collagen fibrils were examined by scanning electron microscopy (SEM) and transmission electron microscopy (TEM). Under SEM, the differences in the size of collagen fibrils were not obvious. In contrast, the gaps between collagen fibrils were reduced in the LAP/VL and RF/UVA groups compared with the CTRL group (Fig. 3a). The structures of collagen fibrils were analyzed more closely in high-magnification TEM images. Corneal stroma comprises thin collagen fibrils embedded in a hydrated proteoglycan matrix. After CXL, the stiffness of the cornea stroma is determined not only by the cross-links between collagen fibrils but also those between and/or proteoglycans [18]. More diffuse amorphous material between collagen fibrils was observed in the LAP/VL and RF/UVA group, which might be due to the emergence of new cross-links between collagen fibrils and/or proteoglycans (indicated by yellow triangles, Fig. 3b). Moreover, the distribution of collagen fibril diameters generated by sampling from 400–900 collagen fibrils revealed a small but statistically significant increase in collagen fibril diameter: the median collagen fibril diameter was 32.19 nm in the CTRL group, 34.89 nm in the LAP/VL group, and 35.25 nm in the RF/UVA group (Fig. 3c and d). In addition, the collagen fibril density displayed a trend of increase in LAP/VL group (Fig. 3e), and the interfibrillar spacing (IFS), which is the center-to-center distance between two adjacent fibrils, was slightly reduced in LAP/VL group compared to CTRL group (Fig. 3f).

The results indicated that LAP/VL treatment could effectively increase the stiffness and rigidity of rabbit corneas *in vivo*, which might be due to the newly-formed links between cornea collagens and/or proteoglycans, and thus altering the ultrastructure of cornea collagen fibrils. In addition to comparable CXL efficiencies, LAP/VL treatment outcompeted RF/UVA protocol as better light transmittance was preserved in cornea.

3.5. Short-term cross-linking effects of LAP/VL in rabbits

Next, changes in collagen microstructure and organization were monitored by IVCM at different depths of corneal stroma [19]. While only stromal cell nuclei backscattered the light under IVCM in the CTRL group, necrotic or apoptotic "ghost cells" [20] were present in the anterior stroma at about 0–100 μm depth in the LAP/VL and RF/UVA group (Fig. 4a). Posterior to these "ghost cells", elongated needle-like structures and hyper-reflective band-like structures were observed sequentially in the middle stroma of both LAP/VL and RF/UVA groups (indicated by the red arrows, Fig. 4a), which might be either migratory corneal fibroblasts or parallel and interlacing collagen lamellae after CXL. At about 300–400 μm depth, a monolayer of highly organized hexagonal endothelial cells was observed in CTRL eyes (Fig. 4a). Although the cell density was not altered, the cell borders were blurred, and few pleomorphic cells were present in the LAP/VL group after CXL. At the same depth, endothelial cells could not be observed in the RF/UVA group because of corneal edema (Fig. 4a).

In addition, to further verify the CXL efficacy *in vivo*, the rabbits were evaluated by anterior segment optical coherence tomography (AS-OCT) on day 10 after surgery. A demarcation line (DL), which defines a transition zone between the cross-linked anterior corneal stroma and the untreated posterior corneal stroma, is considered as an indicator of the depth of CXL treatment and a possible assessment of the effectiveness of the CXL [21]. As expected, a DL was absent in the CTRL group, but it was observed by AS-OCT in the cornea of both LAP/VL and RF/UVA groups (Fig. 4b). The quantification results showed that the DL depth in the LAP/VL group was slightly deeper than that in the RF/UVA group. Still, the discrepancy was not statistically significant (Fig. 4c). Moreover, the overall thickness of corneas was similar between the LAP/VL group and the CTRL group. The value of this parameter was almost doubled in the RF/UVA group on day 10 after CXL (Fig. 4d), indicating a long-lasting and severe cornea edema after RF/UVA treatment.

Therefore, compared with the RF/UVA treatment, the LAP/VL protocol caused less damage to corneal tissues, and a quicker recovery rate was observed in the LAP/VL group.

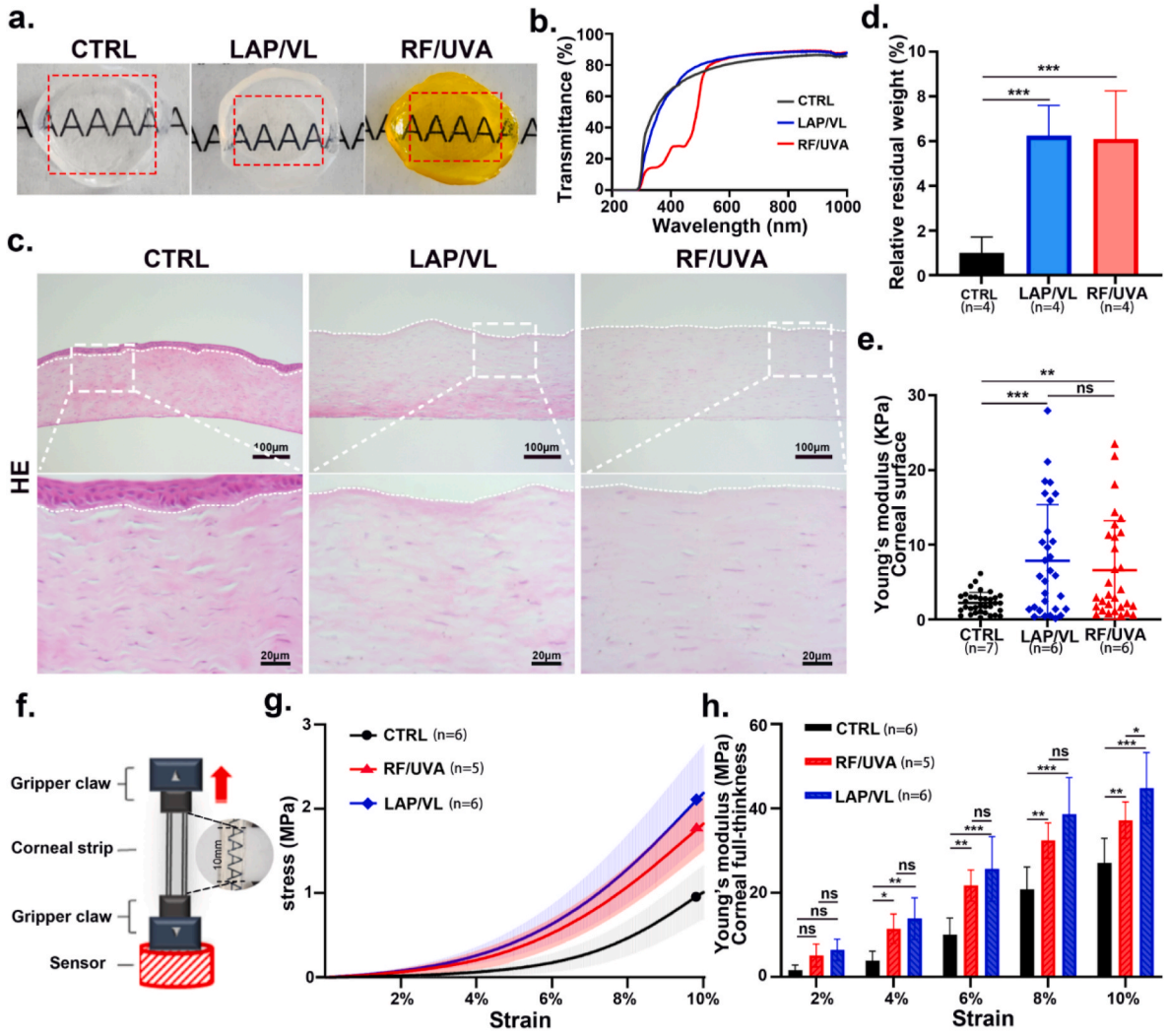

Fig. 2. (a) Rabbit corneal transparency with or without cross-linking. (b) Light transmittance curve in corneas with or without crosslinking. (c) Histological images of rabbit cornea after HE staining. (d) Relative residual corneal weight after collagenase digestion. (e) Young's modulus of rabbit corneal surface was assessed by an atomic force microscope. (f) Illustration of stress-strain tensile test of corneal strips. (g) Stress-strain curves of rabbit corneal strips with or without cross-linking. (h) In tensile testing, instantaneous Young's modulus of full-thickness corneal strips was calculated at 2 %, 4 %, 6 %, 8 %, and 10 % strain. Data are expressed as mean ± S.D., and the number of animals (n) used is labeled in each figure. *$P < 0.05$, **$P < 0.01$, ***$P < 0.001$, for tensile testing, quantification results are analyzed by two-way ANOVA with post-hoc Tukey's test, and other quantification results are analyzed by one-way ANOVA with post-hoc Tukey's test.

Table 3
Young's Modulus of the corneal surface in New Zealand white rabbits after *in vivo* CXL.

	CTRL	LAP/VL	RF/UVA
Corneal numbers	**7**	**6**	**6**
Measure point	**105**	**90**	**90**
Young's modulus (KPa)	**2 ± 1**	**8 ± 8**	**7 ± 7**

Table 4
Young's modulus of corneal strips with or without cross-linking. * Indicates *P* value compared CTRL group with LAP/VL group. *:$P < 0.05$, **: $P < 0.01$, ***: $P < 0.001$, # Indicates *P* value compared CTRL group with RF/UVA group. #: $P < 0.05$, ##: $P < 0.01$, ###: $P < 0.001$, †Indicates *P* value compared to the LAP/VL group with the RF/UVA group. †: $P < 0.05$, ††: $P < 0.01$, †††: $P < 0.001$, Data are expressed as mean ± S.D., one-way ANOVA with post-hoc Tukey's test.

	CTRL	LAP/VL	RF/UVA
Young's modulus at 0 % (MPa)	**1 ± 1**	**4 ± 2**	**3 ± 2**
Young's modulus at 2 % (MPa)	**2 ± 1**	**6 ± 3**	**5 ± 3**
Young's modulus at 4 % (MPa)	**4 ± 2**** #	**14 ± 5****	**11 ± 3**#
Young's modulus at 6 % (MPa)	**10 ± 4***** ##	**26 ± 8*****	**22 ± 4**##
Young's modulus at 8 % (MPa)	**21 ± 5***** ##	**39 ± 9*****	**32 ± 4**##
Young's modulus at 10 % (MPa)	**27 ± 6***##**	**45 ± 8***†**	**37 ± 4**##†

3.6. Long-term cross-linking effects of LAP/VL in rabbits

Furthermore, rabbits were evaluated at 6 weeks after treatment to determine the long-term CXL effectiveness of the LAP/VL protocol. Under IVCM, the enlarged rod-like and interlacing band-like structures remained in the LAP/VL treated cornea. At the same time, endothelial cells returned to typical hexagonal morphologies and organization (Fig. 5a). Both slit-lamp and AS-OCT revealed the persistence of DL in the rabbit cornea from the LAP/VL group (Fig. 5b and c). The relative depth of DL in the LAP/VL group was more than 200 μm (Fig. 5d). However, corneal leucoma and ulcer began to appear from day 7 in the RF/UVA group after CXL (Fig. S3), which hindered further laboratory and clinical examinations. At 6 weeks, the overall corneal thickness in the LAP/VL group was similar to that of the CTRL group (Fig. 5e). Additionally, the stiffness of the cornea was re-evaluated by AFM indentation. The Young's modulus was 4 ± 2 kPa for the LAP/VL group

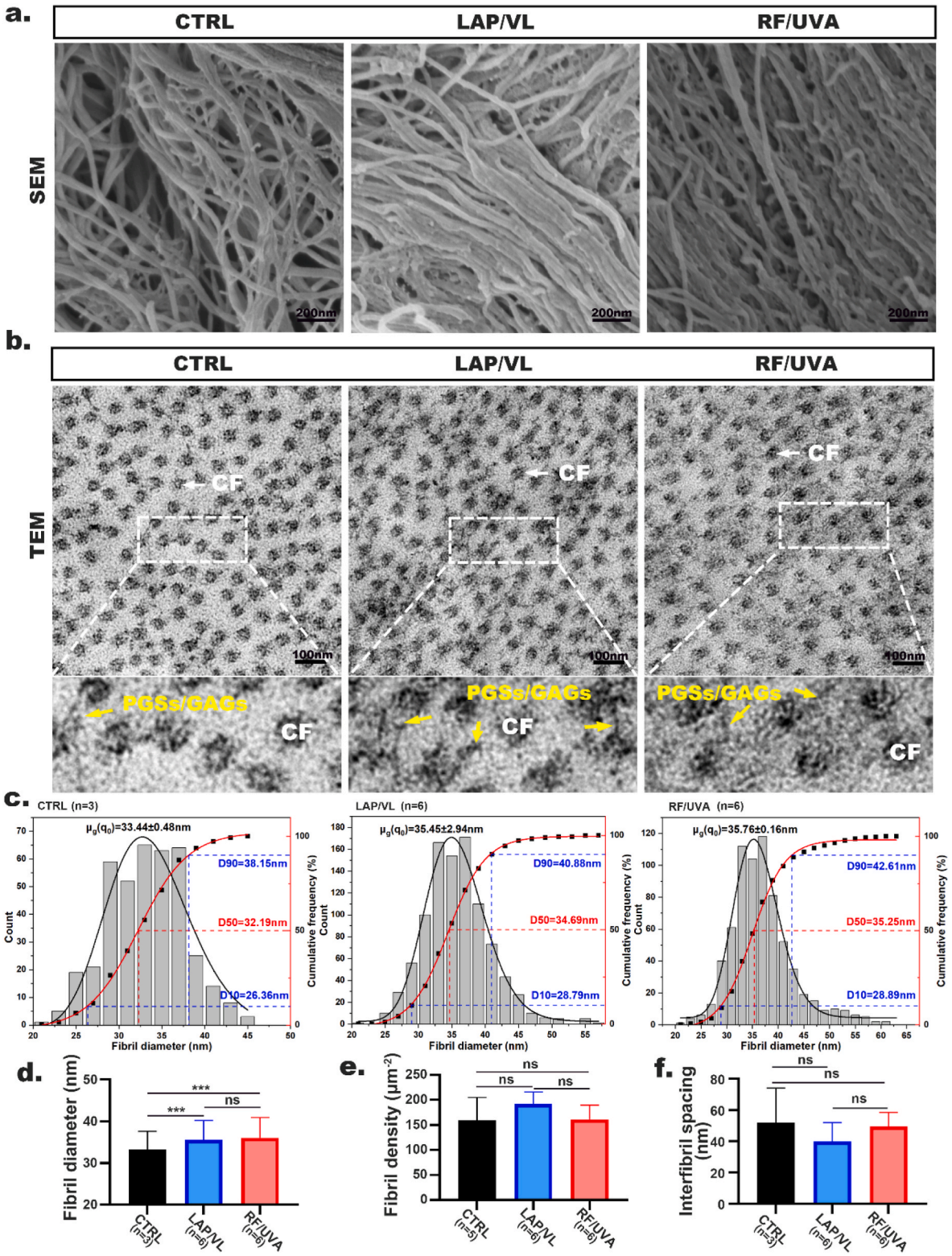

Fig. 3. (a) Representative scanning electron microscopy (SEM) images of collagen fibrils in the superficial stroma layer of rabbit cornea with or without cross-linking. (b) Representative transmission electron microscopy (TEM) images of rabbit corneal collagen fibrils obtained from the anterior part of the cornea. CF: collagen fibrils; PGSs: proteoglycans; GAGs: glycosaminoglycan. (c) Distribution of collagen fibril diameters in the superficial stromal layer. Quantification of collagen fibril diameter (d), fibril density (e), and interfibrillar spacing (f). The collage fibril diameter data are expressed as median ± S.D. , and other data are expressed as mean ± S.D., and the number of animals (n) used is labeled in each figure. *$P < 0.05$, **$P < 0.01$, ***$P < 0.001$, one-way ANOVA with post-hoc Tukey's test.

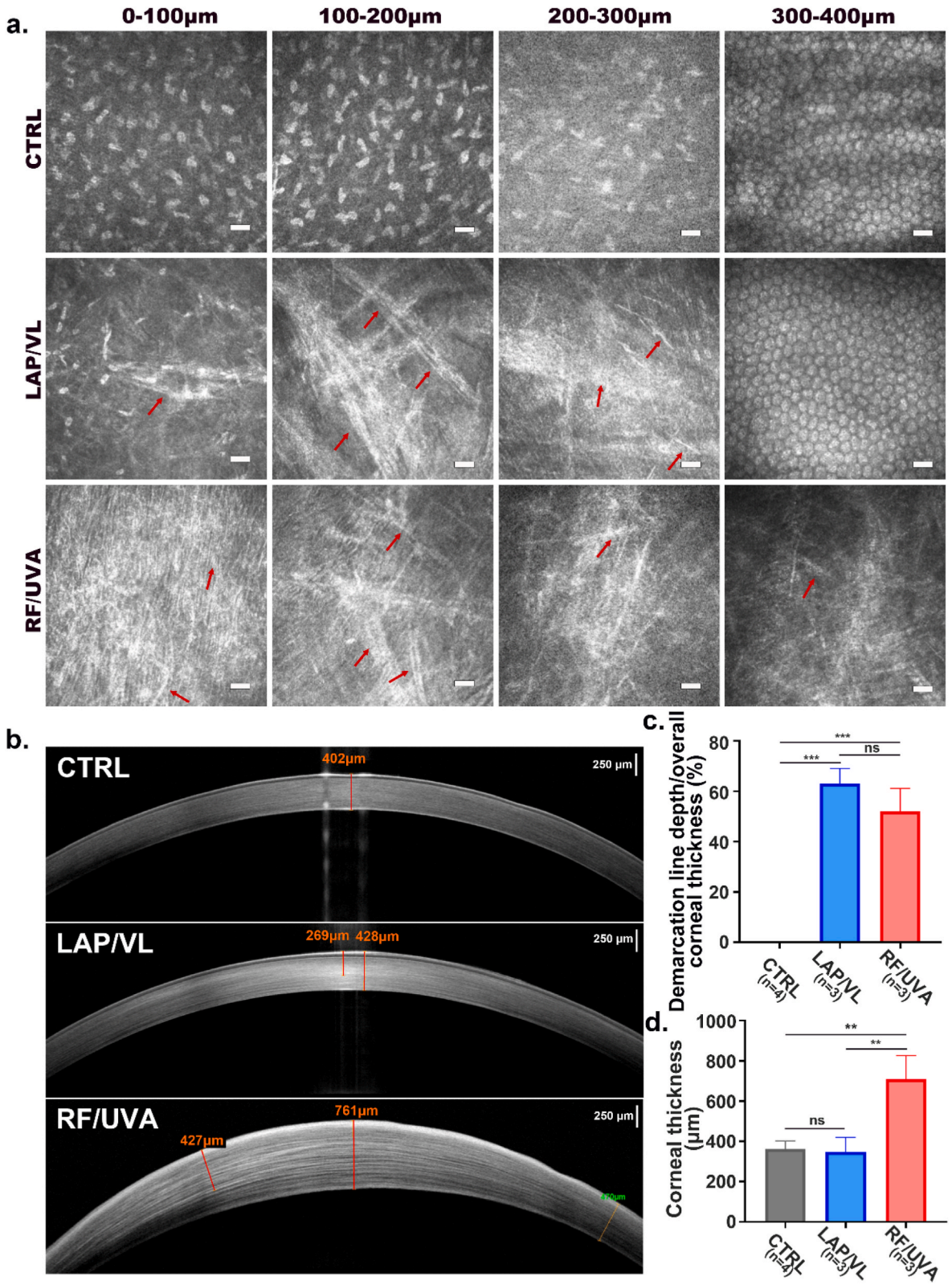

Fig. 4. (a) Representative *in vivo* corneal confocal microscopy (IVCM) images at different depths of rabbit cornea at 10 d after cross-linking. The changes in collagen fibril after cross-linking are indicated by red arrows (scale bar = 50 μm). (b) Representative anterior segment optical coherence tomography (AS-OCT) images of rabbit cornea with or without cross-linking. Quantification of relative demarcation line depth (c) and overall corneal thickness (d) based on AS-OCT images obtained 10 d after cross-linking. Data are expressed as mean ± S.D., and the number of animals (n) used is labeled in each figure. $^{*}P < 0.05$, $^{**}P < 0.01$, $^{***}P < 0.001$, one-way ANOVA with post-hoc Tukey's or Sidak's test. (For interpretation of the references to color in this figure legend, the reader is referred to the Web version of this article.)

and 2 ± 1 kPa for the CTRL group (Fig. 5f–Table 5, $p < 0.0001$).

All these data suggested that LAP/VL treatment could effectively increase the corneal rigidity for at least 6 weeks. Because the thickness of rabbit cornea is less than or around 400 μm (the safety threshold of standard RF/UVA treatment), complications, including persistent cornea edema, leucoma, and even corneal ulcers were observed. Encouragingly, all these complications were absent in the LAP/VL treated cornea, suggesting an improved safety of the LAP/VL protocol for relatively thin cornea CXL.

Table 5
Young's Modulus of corneal stroma surface in rabbits on the 6th week after CXL surgery.

	CTRL	LAP/VL
Corneal numbers	**4**	**5**
Measure point	**60**	**75**
Young's modulus (KPa)	**2 ± 1**	**4 ± 2**

3.7. Biocompatibility of LAP/VL protocol in rabbits

To further evaluate the biocompatibility of LAP/VL treatment, primary human corneal stromal cells (HCSC) were extracted from

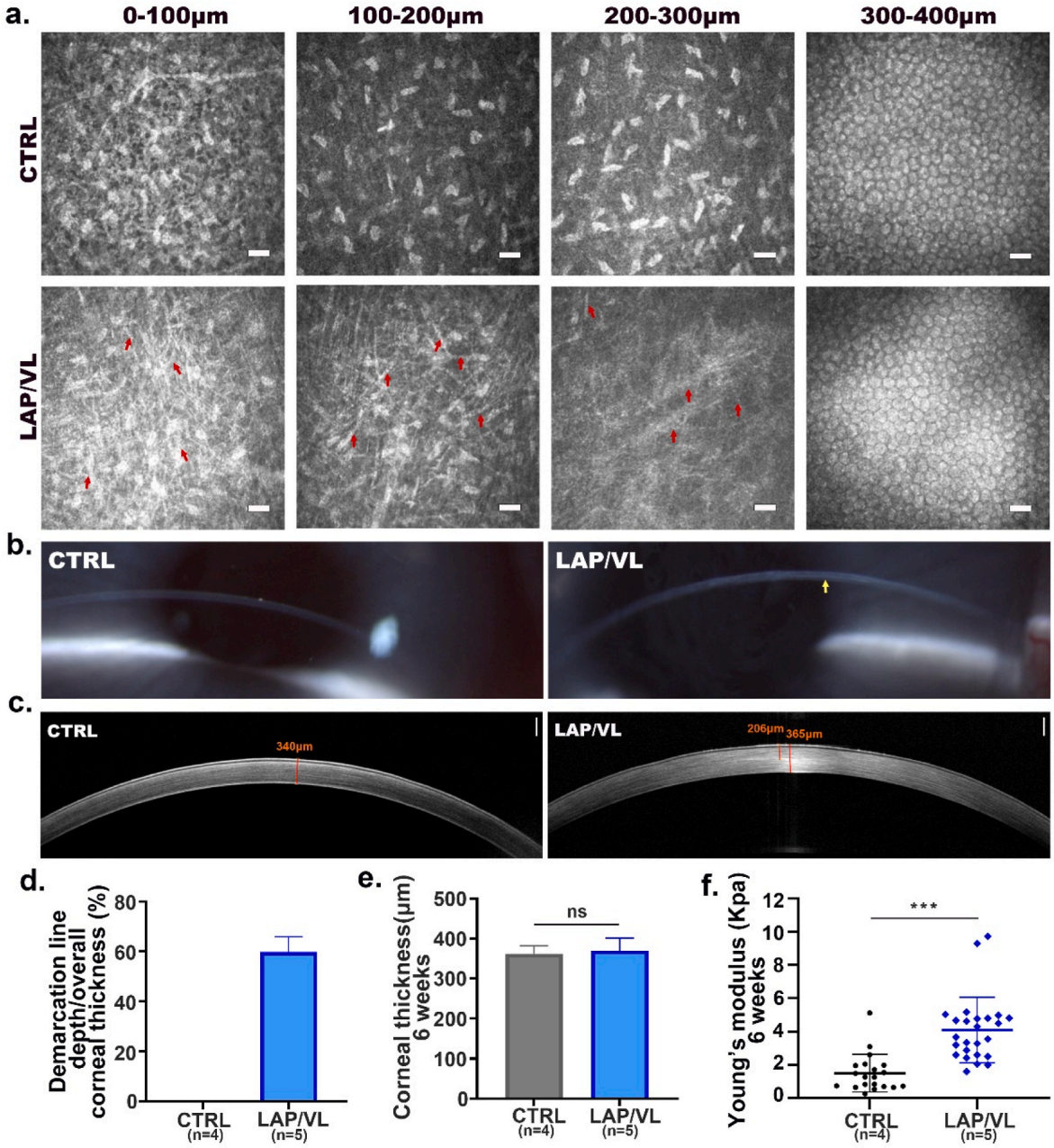

Fig. 5. (a) Representative IVCM images of rabbit cornea at different depths 6 weeks after corneal cross-linking. Red arrows indicate the long-lasting changes in collagen fibrils (scale bar = 50 μm). (b) Representative slit-lamp images of rabbit cornea at 6 weeks after corneal cross-linking. The presence of a demarcation line after cross-linking is indicated by the yellow arrow. (c) Representative AS-OCT images of rabbit cornea at 6 weeks after corneal cross-linking. Quantification of relative demarcation line depth (d), overall corneal thickness (e), and corneal surface Young's modulus evaluated by atomic force microscope (f) at 6 weeks after corneal cross-linking. Data are expressed as mean ± S.D., and the number of animals (n) used is labeled in each figure. $^{*}P < 0.05$, $^{**}P < 0.01$, $^{***}P < 0.001$, unpaired student's *t*-test. (For interpretation of the references to color in this figure legend, the reader is referred to the Web version of this article.)

keratoconus patients' corneal buttons after keratoplasty and cultured for cell toxicity experiments. After co-culturing HCSC with different concentrations of LAP or 0.25 % RF for 24 h, cell viabilities were not reduced in all treated groups (Fig. 6a). Moreover, live/dead cell staining showed no PI-positive dead cells after treatment with 0.25 % LAP or 0.25 % RF for 24 h (Fig. 6b). Both results confirmed the biocompatibility of LAP to corneal stroma cells without irradiation.

In rabbit models, the corneal epithelium wound healing rates were evaluated by fluorescein staining under slit-lamp for consecutive 5 days after surgery. Although the corneal epithelial wound was healed by 4 days for both LAP/VL and RF/UVA groups, the wound closure rate was similar between the LAP/VL group and RE-CTRL group (sham group only removing corneal epithelium), and both were significantly faster than that of the RF/UVA group (Fig. 6c and d). The debridement of corneal epithelium and CXL surgery caused stromal edema in both LAP/VL and RF/UVA groups. Although it was quickly resolved within 5 days after CXL in the LAP/VL group, cornea edema persisted in the RF/UVA group (Fig. 6c and e), suggesting more severe damage to cornea cells after RF/UVA treatment. Consistently, slit-lamp microscopy revealed significant and persistent corneal edema in the RF/UVA group (Fig. 6e), and overall cornea thickness was about 2-fold thicker in the RF/UVA group than in the LAP/VL group (Fig. 6f).

A monolayer of corneal endothelium lines the posterior surface of the cornea, and it functions as a barrier between the corneal stroma and aqueous humor to maintain stromal deturgescence [22]. Moreover, corneal endothelium expresses many ion pumps, which move water osmotically from the stroma into the aqueous humor [22]. Therefore, loss of corneal endothelial cells is the leading cause of corneal edema. During CXL, UVA exposure stimulates riboflavin into a triplet state, which generates reactive oxygen species (ROS). Irradiating the cornea with UVA could also produce ROS in the aqueous humor [23]. Although ROS generation is critical for cross-links formation between collagen fibrils/proteoglycans, it also leads to irreversible damage to corneal endothelium [22b]. Accordingly, corneal tissues were collected immediately after surgery to stain with 8-OHdG (a marker for DNA oxidative damage) and γH2AX (a marker for DNA double-strand break). The fluorescence intensities for both markers were significantly increased in RF/UVA treated endothelium (Fig. 7a–d), suggesting the RF/UVA protocol caused oxidative DNA damage in corneal endothelium because of the thin cornea in rabbits. The integrity of the corneal endothelium was evaluated by the wholemount staining of tight junction protein ZO-1. ZO-1 staining showed a uniform and integral structure of hexagonal endothelial cells in the CTRL group. There were few cells with reduced and blurred ZO-1 expression in the borders of endothelial cells after LAP/VL treatment. In contrast, many cells had lost regular endothelial morphology in the RF/UVA group (Fig. 7e).

To further confirm severe cornea damage caused by the RF/UVA protocol, corneal tissues were collected 3 d after CXL. H&E staining showed that the corneal stroma of the LAP/VL group was more densely packed than the CTRL group on the 3rd d after CXL, and 2–3 layers of epithelial cells fully covered the corneal surface (Fig. 8a). In contrast, the corneal stroma was much thicker in the RF/UVA group than in the CTRL and LAP/VL groups, and the regenerated epithelial cells were unable to cover the corneal surface (Fig. 8a). Stromal cells were observed in the anterior CTRL cornea, the number of stromal cells was reduced after LAP/VL treatments, and complete loss of stromal cells was observed in the cornea of the RF/UVA group (Fig. 8a and b). In line with the findings immediately after CXL, the wholemount staining of ZO-1 showed that the endothelial integrity was severely damaged by RF/UVA treatment but not LAP/VL treatment (Fig. 8c and d). On day 3 after CXL, more severe alterations of cornea endothelium were observed in the RF/UVA cornea, suggesting a progressive and irreversible degeneration of endothelial cells. The cell number and pump functions of endothelial cells determine the ability of endothelium to remove extra fluid from the cornea [24]. Thus, wholemount staining of Na^+/K^+ ATPase was used to measure the pump functions of the endothelium after CXL. Similar to the results of ZO-1 staining, RF/UVA treatment was associated with deterioration in the expression of Na^+/K^+ ATPase (Fig. 8e and f), which explained the persistent cornea edema after RF/UVA CXL.

4. Discussion

Clinically, the patient's preoperative corneal thickness is recommended to be no less than 400 μm when the standard CXL protocol (also known as the Dresden protocol) is used, and the primary purpose of this requirement is to protect corneal endothelium [25]. Unfortunately, progressive cornea thinning characterizes Keratoconus; thus, patients with moderate-to-advanced corneal ectasia usually cannot meet the prerequisite for standard CXL procedures. It was reported that approximately 25 % of patients with keratoconus had pachymetry readings below 400 μm during their initial clinic visits. [26]. Clinical scientists have developed various solutions to address this issue, such as wearing contact lenses [27], utilizing hypo-osmolar RF solution to increase overall corneal thickness [28], employing transepithelial CXL [29], iontophoresis-assisted CXL [30], and accelerating CXL with high-energy UVA in a short time frame [31]. However, maintaining the balance between CXL efficiency and tissue safety continues to pose a challenge. In this study, we found that the LAP/VL protocol not only effectively cross-linked the cornea, but also protected the endothelium in rabbits (Figs. 7 and 8). This finding strongly supports the effectiveness and safety of the LAP/VL protocol for CXL in relatively thin cornea.

It was reported that RF/visible blue light (435 nm) could cross-link porcine cornea *in vitro*, yet with less efficiencies than RF/UVA strategy [4]. Here, we demonstrated that the LAP/VL protocol could achieve equivalent CXL effectiveness as the RF/UVA protocol in both porcine eyes *in vitro* (Fig. S2, Table S1) and rabbit models *in vivo* (Fig. 2, Tables 3 and 4), suggesting that LAP might be a photosensitizer candidate for corneal CXL in clinics under VL. Since RF has an absorbance peak at 435 nm in the visible light range, the LAP/VL protocol should outcompete RF/VL treatment in corneal CXL.

Corneal CXL is a successful therapeutic application of light-initiated polymerization in the biomedical field. To initiate corneal collagen CXL, a suitable photo-initiator should possess the following properties: high quantum efficiency, good water solubility, non-cytotoxicity, no impact on corneal color and transparency, and thermal-temporal stability [10]. Additionally, to avoid potential tissue damage induced by UVA, we focused on identifying photo-initiators with absorption wavelength in the visible light range. Consequently, two families of photo-initiators, mono-acylophosphine oxides (MAPOs, also known as TPO) and bis-acylophosphine oxides(BAPOs), became candidates for our study. Both TPO salts and BAPO salts meet the requirements. Moreover, they are both commercially available and feature a simple one-pot synthesis procedure [32]. Among them, LAP was selected not only because it exhibits the lowest cytotoxicity and genotoxicity in multiple cell culture models [33], but also because it is colorless and odorless.

In this study, we used LAP in combination with 4.5 mW/cm^2 405 nm light to cross-link rabbit cornea for 20 min, which raises the concern that 405 nm VL may cause damage to the neurosensory retina. While multiple studies demonstrated that excessive light can cause retinal damage through photothermal, photomechanical, and photochemical mechanisms, these effects typically require high-levels of light energy. Previous studies demonstrated that 50 mW/cm^2 light (430±20 nm) irradiation for 30 min only caused retinal degeneration in mice with visual cycle dysfunction but not in wildtype mice [34]. Considering the fact that irradiance and irradiation time used in our study were lower, and that LAP could absorb light in cornea, the LAP/VL protocol induced retinal damage should be neglectable.

According to the Beer-Lambert law, the transparent cornea could be considered as a substance, and the attenuation of light is proportional to the amount of photocatalysts (such as RF or LAP) which can absorb light. Both RF/UVA and LAP/VL protocol could increase corneal strengths to a

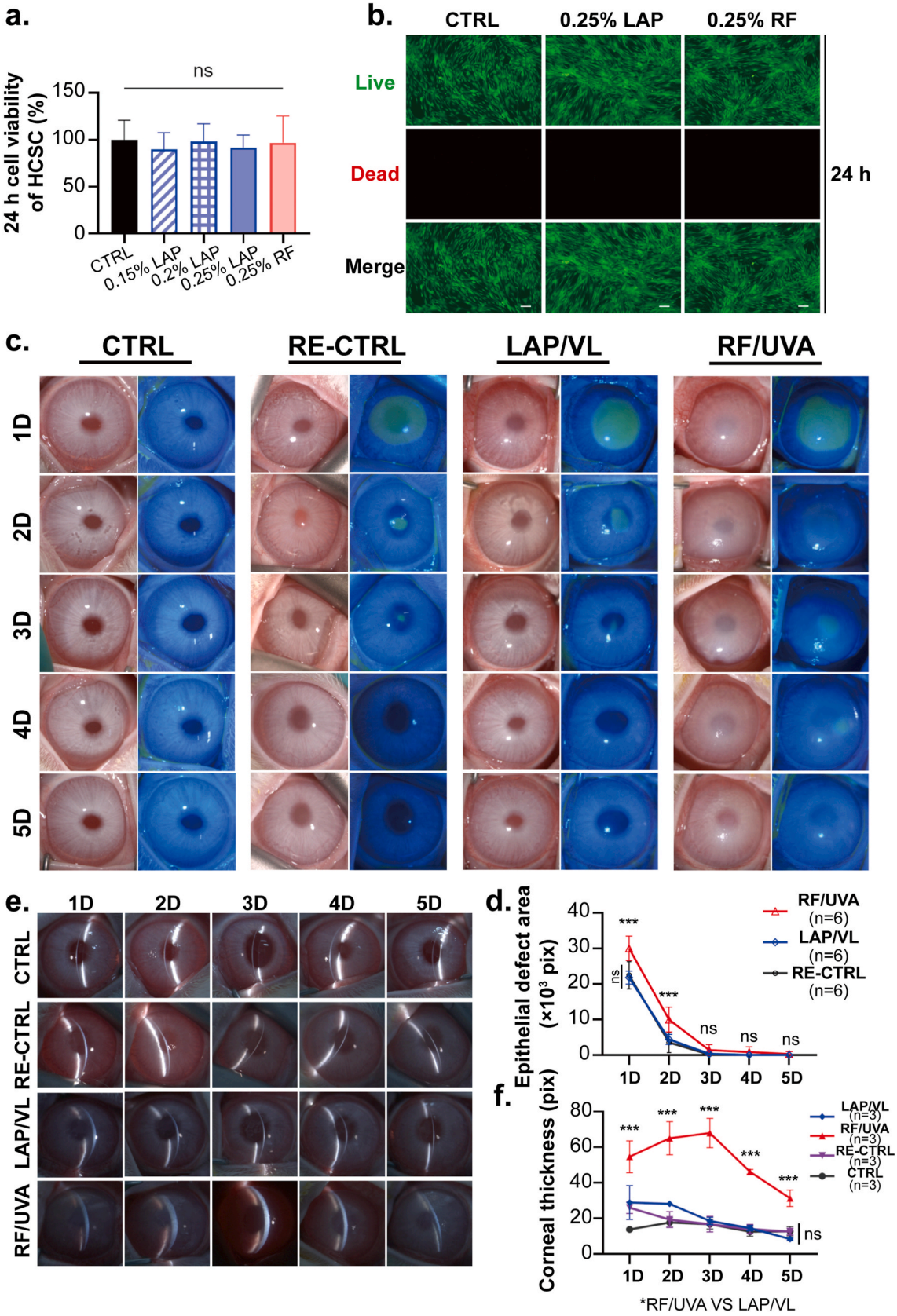

Fig. 6. (a) Cell viability at 24 h after different concentrations of LAP or 0.25 % RF treatment in primary human corneal stromal cells. (b) Live and dead staining of primary human stromal cells at 24 h after 0.25 % LAP and 0.25 % RF treatment (scale bar = 100 μm). Fluorescein staining of corneal epithelium defects (c) and slit-lamp images (e) of rabbit cornea after cross-linking. Quantification of corneal epithelial defect area (d) and overall corneal thickness (f) after corneal cross-linking. Data are expressed as mean ± S.D., and the number of animals (n) used is labeled in each figure. $^{*}P < 0.05$, $^{**}P < 0.01$, $^{***}P < 0.001$, for cell viability assay, data are analyzed by one-way ANOVA with post-hoc Tukey's test, and all other comparisons were analyzed by two-way ANOVA with post-hoc Tukey's or Sidak's test.

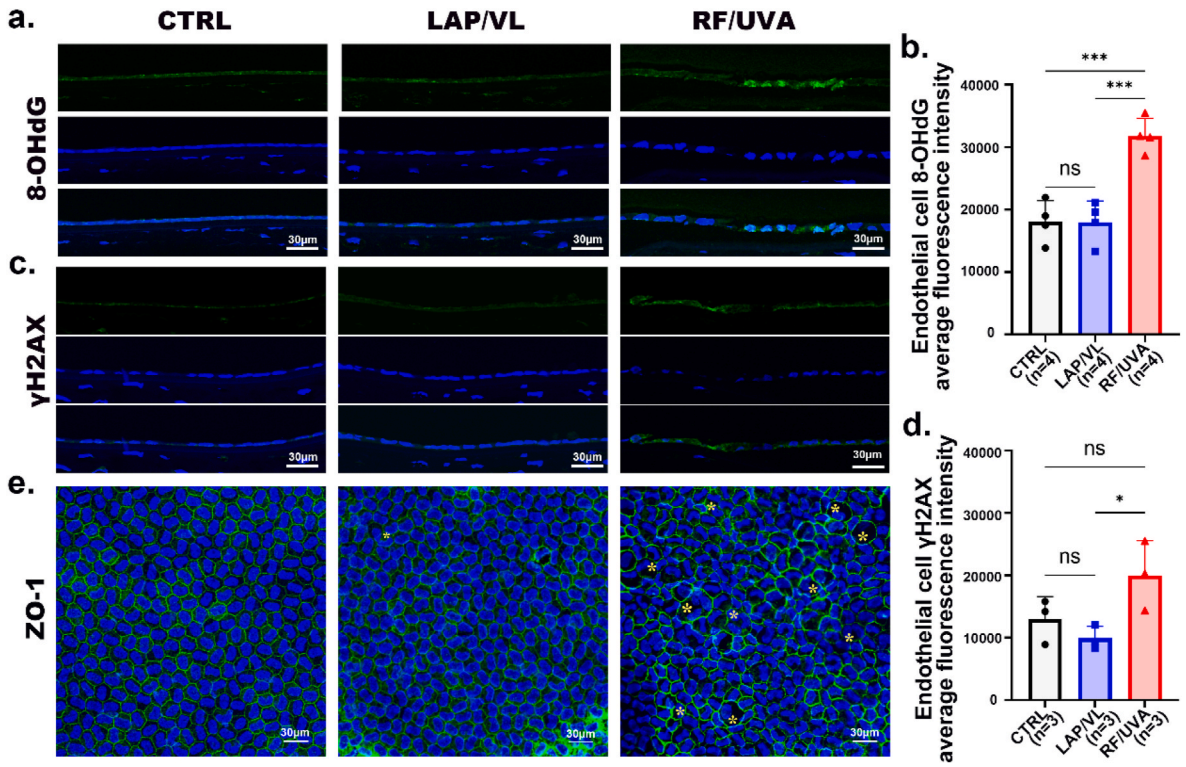

Fig. 7. The immunofluorescence staining and quantification of 8-OHdG (a,b) and γH2AX (c,d) in rabbit cornea immediately after cross-linking. (e) The immunofluorescence staining of zonula occludens protein 1 (ZO-1) in rabbit central corneal endothelium. The yellow asterisk indicates abnormal endothelial cells. Data are expressed as mean ± S.D., and the number of animals (n) used is labeled in each figure. $^{*}P < 0.05$, $^{**}P < 0.01$, $^{***}P < 0.001$, one-way ANOVA with post-hoc Tukey's test. (For interpretation of the references to color in this figure legend, the reader is referred to the Web version of this article.)

similar level (Figs. 2 and 3,S2, Tables 3 and 4,S1), suggesting that the energy transfer capabilities of both methods are comparable. It is well conceived that when RF is used as a photocatalyst, the generation of ROS is critical for CXL reaction, which requires sufficient oxygen supply in corneal tissues. When higher energy is used to accelerate CXL process, the quicker depletion of intrastromal oxygen impedes the reaction. Recently, it was shown that graphitic carbon nitride quantum dots (g-C_3N_4 QDs) could be used as a synergist of photosensitizer RF to improve the CXL efficiency of the accelerated RF/UVA protocol [35]. Theoretically, g-C_3N_4 QDs have abilities to extend the absorbance spectrum of photocatalysts to the visible light range [36]. Thus, it would be interesting to know if VL could efficiently cross-link the cornea when applied simultaneously with riboflavin/g-C_3N_4 QDs. In this study, we found that photo-initiator LAP could effectively cross-link porcine and rabbit cornea under VL, and the impact of this strategy on corneal endothelium integrity (Figs. 4, 7 and 8), epithelial wound healing rate (Fig. 6), and corneal stroma cell loss (Fig. 8) was reduced in comparison with the RF/UVA protocol in the rabbits. The CXL effect and enhanced biocompatibility of the LAP/VL protocol did not necessitate the manipulation of additional microenvironment factors, further supporting its translational potentials.

In addition to CXL efficiency and biocompatibility, it is important to evaluate the long-term CXL effect as well. In this study, corneal edema (Figs. 4 and 6) and haze/leucoma/ulcer (Fig. S3) were observed in the rabbits within two weeks. As a result, we were unable to evaluate the long-term Young's modulus of the rabbit corneal tissues in the RF/UVA group. Interestingly, we found that the strength of corneal stroma after the LAP/VL CXL remained around 1-fold higher than CTRL after 6 weeks following the treatment (Fig. 5), suggesting LAP/VL induced cornea CXL were maintained for a long period. However, a direct comparison between RF/UVA and LAP/VL protocols for long-term CXL effects *in vivo* is interesting. Since more side effects were observed in both rabbit and mouse models, the RF/UVA protocol might cause more severe and irreversible damages to corneal tissues than the LAP/VL protocol under comparable conditions. Thus, we propose that the LAP/VL protocol could be a safer strategy to cross-link cornea, especially for patients with advanced corneal ectasia diseases.

A limitation in this study is that we used rabbits as the models. Firstly, the central cornea thickness of 2.5 kg rabbits is less than 400 μm [37], and cornea shrinkage occurs after RF application [8], which further reduces the corneal thickness. Secondly, rabbit corneal endothelial cells possess regenerative capacity, which might mask the damage induced by the LAP/VL protocol. Therefore, the safety and efficacy of the LAP/VL protocol require future validation in human corneas. The standard Dresden protocol employs 0.1 % (w/v) RF for corneal CXL. Another limitation is that this study used 0.25 % (w/v) RF in the reference group, which might lead to higher concentration of RF at the endothelial level and increased ROS generation after UVA irradiation, and exaggerate endothelial cell death after CXL. Therefore, the side effects of the RF/UVA protocol might be overestimated.

5. Conclusions

In summary, our results demonstrated that the combination of water-soluble photo-initiators LAP and visible light (VL) irradiation could effectively cross-link native stromal collagens in both porcine and rabbit corneas, achieving equivalent or even slightly better CXL results compared with the standard RF/UVA protocol. More importantly, the LAP/VL protocol could preserve corneal endothelium integrity and functionality, reduce the death of corneal stroma cells under the comparable condition, and promote more rapid closure of corneal epithelium wounds; and thus decrease the incidence of corneal edema, haze, or

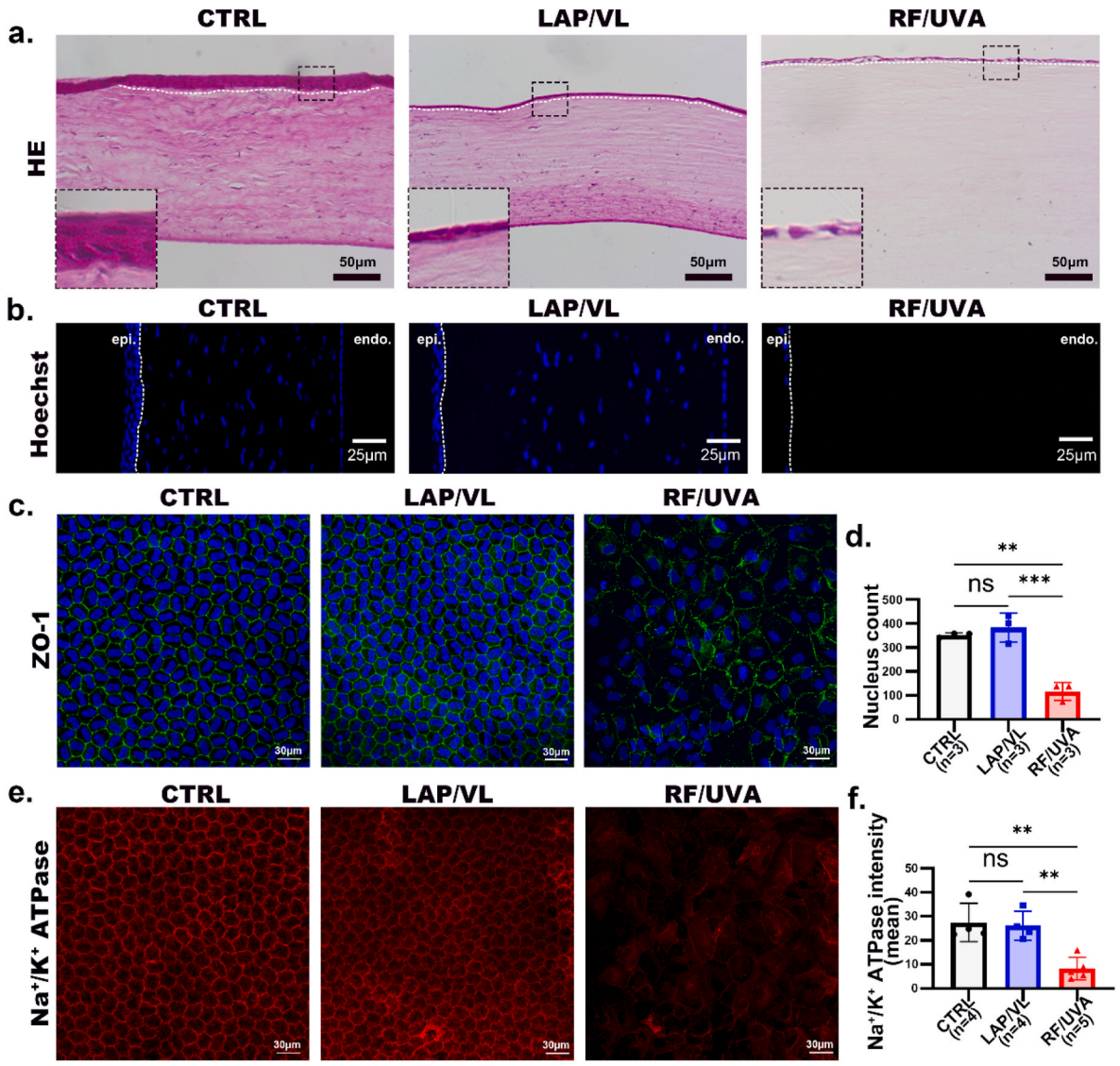

Fig. 8. (a) Histological images of rabbit cornea on the 3rd d after cross-linking. (b) Hoechst staining of rabbit cornea sections at 3 d after cross-linking. epi: epithelium; endo: endothelium. The immunofluorescence staining and quantification of ZO-1 (c,d) and Na^+/K^+ ATPase (e,f) 3 d after cross-linking. Data are expressed as mean ± S.D., and the number of animals (n) used is labeled in each figure. $^*P < 0.05$, $^{**}P < 0.01$, $^{***}P < 0.001$, one-way ANOVA with post-hoc Tukey's test.

ulcer after corneal cross-linking. Based on our experimental findings, we propose that LAP/VL protocol has potentials for relatively thin cornea cross-linking, which is worth further investigation. Our study expands the application scope of LAP, supporting its capabilities for *in vivo* tissue engineering and therapies.

CRediT authorship contribution statement

Yi Liao: Writing – review & editing, Writing – original draft, Supervision, Methodology, Investigation, Funding acquisition, Conceptualization. **Shengmei Zhou:** Writing – original draft, Visualization, Methodology, Investigation, Formal analysis. **Andrew J. Quantock:** Methodology, Funding acquisition, Data curation. **Wei Li:** Methodology, Data curation. **Yuan Xu:** Investigation. **Xie Fang:** Resources, Methodology. **Robert D. Young:** Validation, Methodology, Investigation. **Wanling He:** Investigation. **Qingjian Li:** Investigation. **Houjian Zhang:** Methodology. **Ruochen Wang:** Project administration, Methodology. **Yi Han:** Methodology. **Hongwei Cheng:** Methodology. **Wenjun Li:** Resources. **Lu Peng:** Resources. **Rongrong Zong:** Project administration. **Yi Hong:** Methodology, Conceptualization. **Zhirong Lin:** Writing – review & editing, Supervision, Resources, Methodology, Conceptualization. **Zuguo Liu:** Supervision, Funding acquisition.

Data availability statement

The raw/processed data required to reproduce these findings will be shared upon proper request.

Declaration of competing interest

The authors declare that they have no known competing financial interests or personal relationships that could have appeared to influence the work reported in this paper.

Acknowledgment

This work was supported by grants from National Key R&D Program of China (2019YFA0111200) and the Natural Science Foundation of Xiamen, China (3502Z202373024), Xiamen Health High-quality Development Science and Technology Program (2024GZL-ZD14),

Fujian Province Innovation and Entrepreneurship Talents (2021), Fujian Provincial Science Fund (2023J011589), Fujian Provincial Health Technology Project (2022GGB023), and MRC programme Grant (MR/S037829/1). We thank Qingfeng Liu (Core Facility of Biomedical Sciences, Xiamen University) for help with atomic force microscopy. We thank Luming Yao, Caiming Wu, and Wei Han (State Key Laboratory of Cellular Stress Biology, School of Life Sciences, Xiamen University) for their help with electron microscopy. We thank Jingru Huang and Xiang You from Central Lab, School of Medicine, Xiamen University, for their technical support in confocal imaging. We thank Dr. Sally Hayes from School of Optometry and Vision Sciences, Cardiff University, for insightful discussion with collagenase resistance experiments, Dr. Chengchao Chu from School of Medicine, Xiamen University for insightful suggestions.

Appendix A. Supplementary data

Supplementary data to this article can be found online at https://doi.org/10.1016/j.mtbio.2025.102110.

Data availability

Data will be made available on request.

References

[1] J. Chong, W.J. Dupps Jr., Exp. Eye Res. 205 (2021) 108508.
[2] R.P.C. Manns, A. Achiron, B. Knyazer, O. Elhaddad, K. Darcy, T. Yahalomi, D. Tole, V.S. Avadhanam, Graefes Arch. Clin. Exp. Ophthalmol. 261 (2023) 2435.
[3] E. Koudouna, E. Mikula, D.J. Brown, R.D. Young, A.J. Quantock, J.V. Jester, Acta Biomater. 79 (2018) 96.
[4] .
E. Spörl, M. Huhle, M. Kasper, T. Seiler, Ophthalmologe 94 (1997) 902;
b) E. Spoerl, M. Huhle, T. Seiler, Exp. Eye Res. 66 (1998) 97.
[5] a) G. Wollensak, E. Spoerl, T. Seiler, Am. J. Ophthalmol. 135 (2003) 620;
b) J.B. Randleman, S.S. Khandelwal, F. Hafezi, Surv. Ophthalmol. 60 (2015) 509.
[6] A.M. Hagem, A. Thorsrud, M. Sæthre, G. Sandvik, O. Kristianslund, L. Drolsum, Cornea (2023).
[7] T.L. de Jager, A.E. Cockrell, S.S. Du Plessis, Adv. Exp. Med. Biol. 996 (2017) 15.
[8] T.G. Seiler, A. Batista, B.E. Frueh, K. Koenig, Investig. Ophthalmol. Vis. Sci. 60 (2019) 2140.
[9] S. Reischauer, B. Pieber, iScience 24 (2021) 102209.
[10] W. Tomal, J. Ortyl, Polymers 12 (2020).
[11] T. Majima, W. Schnabel, W. Weber, Makromol. Chem. 192 (1991).
[12] B.D. Fairbanks, M.P. Schwartz, C.N. Bowman, K.S. Anseth, Biomaterials 30 (2009) 6702.
[13] a) N. Bouheraoua, L. Jouve, M. El Sanharawi, O. Sandali, C. Temstet, P. Loriaut, E. Basli, V. Borderie, L. Laroche, Investig. Ophthalmol. Vis. Sci. 55 (2014) 7601;
b) X. Wang, J. Dong, Q. Wu, Vet. Ophthalmol. 17 (2014) 87.
[14] S. Hayes, C.S. Kamma-Lorger, C. Boote, R.D. Young, A.J. Quantock, A. Rost, Y. Khatib, J. Harris, N. Yagi, N. Terrill, K.M. Meek, PLoS One 8 (2013) e52860.
[15] R.W. Lewis, J.C. McCall, P.A. Botham, R. Trebilcock, Toxicol. Vitro 8 (1994) 867.
[16] Z. Zhao, M. Liang, H. He, X. Wang, C. Zhu, L. Li, B. Liu, R. Zong, Q. Jin, H. Wu, W. Li, Z. Lin, Front. Med. 9 (2022) 762730.
[17] K.M. Meek, D.W. Leonard, Biophys. J. 64 (1993) 273.
[18] a) H. Hatami-Marbini, M.E. Emu, Exp. Eye Res. 231 (2023) 109476;
b) H. Hatami-Marbini, M.E. Emu, Exp. Eye Res. 234 (2023) 109570.
[19] C. Jordan, D.V. Patel, N. Abeysekera, C.N. McGhee, Ophthalmology 121 (2014) 469.
[20] W.M. Petroll, M. Miron-Mendoza, Y. Sunkara, H.R. Ikebe, N.R. Sripathi, H. Hassaniardekani, Exp. Eye Res. 233 (2023) 109523.
[21] a) T. Seiler, F. Hafezi, Cornea 25 (2006) 1057;
b) L. Spadea, E. Tonti, E.M. Vingolo, Clin. Ophthalmol. 10 (2016) 1803.
[22] a) W.M. Bourne, Eye (Lond) 17 (2003) 912;
b) T. Schmedt, M.M. Silva, A. Ziaei, U. Jurkunas, Exp. Eye Res. 95 (2012) 24.
[23] C. Liu, T. Miyajima, G. Melangath, T. Miyai, S. Vasanth, N. Deshpande, V. Kumar, S. Ong Tone, R. Gupta, S. Zhu, D. Vojnovic, Y. Chen, E.G. Rogan, B. Mondal, M. Zahid, U.V. Jurkunas, Proc. Natl. Acad. Sci. U. S. A. 117 (2020) 573.
[24] S. Hatou, Cornea 30 (Suppl 1) (2011) S60.
[25] a) B. Bagga, S. Pahuja, S. Murthy, V.S. Sangwan, Cornea 31 (2012) 1197;
b) A. Sharma, J.M. Nottage, K. Mirchia, R. Sharma, K. Mohan, V.S. Nirankari, Am. J. Ophthalmol. 154 (2012) 922;
c) M.W. Belin, L. Lim, R.K. Rajpal, F. Hafezi, J.A.P. Gomes, B. Cochener, Cornea 37 (2018) 1218.
[26] Y. Han, Y. Xu, W. Zhu, Y. Liu, Z. Liu, X. Dou, G. Mu, J Ophthalmol 2017 (2017) 6490915.
[27] S. Jacob, D.A. Kumar, A. Agarwal, S. Basu, P. Sinha, A. Agarwal, J. Refract. Surg. 30 (2014) 366.
[28] F. Hafezi, M. Mrochen, H.P. Iseli, T. Seiler, J. Cataract Refract. Surg. 35 (2009) 621.
[29] F. Hafezi, Cornea 41 (2022) 1203.
[30] R. Vinciguerra, E.F. Legrottaglie, C. Tredici, C. Mazzotta, P. Rosetta, P. Vinciguerra, J. Clin. Med. 11 (2022).
[31] F. Hafezi, S. Kling, F. Gilardoni, N. Hafezi, M. Hillen, R. Abrishamchi, J.A. P. Gomes, C. Mazzotta, J.B. Randleman, E.A. Torres-Netto, Am. J. Ophthalmol. 224 (2021) 133.
[32] H. Wang, B. Zhang, J. Zhang, X. He, F. Liu, J. Cui, Z. Lu, G. Hu, J. Yang, Z. Zhou, R. Wang, X. Hou, L. Ma, P. Ren, Q. Ge, P. Li, W. Huang, ACS Appl. Mater. Interfaces 13 (2021) 55507.
[33] a) S. Benedikt, J. Wang, M. Markovic, N. Moszner, K. Dietliker, A. Ovsianikov, H. Grützmacher, R. Liska, J. Polym. Sci., Part A: Polym. Chem. 54 (2016) 473;
b) M. Popal, J. Volk, G. Leyhausen, W. Geurtsen, Dent. Mater. 34 (2018) 1783.
[34] L. Wu, K. Ueda, T. Nagasaki, J.R. Sparrow, Investig. Ophthalmol. Vis. Sci. 55 (2014) 1910.
[35] M. Yang, T. Chen, X. Chen, H. Pan, G. Zhao, Z. Chen, N. Zhao, Q. Ye, M. Chen, S. Zhang, R. Gao, K.M. Meek, S. Hayes, X. Ma, X. Li, Y. Wu, Y. Zhang, N. Kong, W. Tao, X. Zhou, J. Huang, Nat. Commun. 15 (2024) 5508.
[36] M. Majdoub, D. Sengottuvelu, S. Nouranian, A. Al-Ostaz, ChemSusChem 17 (2024) e202301462.
[37] A.K. Riau, N.Y. Tan, R.I. Angunawela, H.M. Htoon, S.S. Chaurasia, J.S. Mehta, BMC Vet. Res. 8 (2012) 138.